Radiation defect dynamics in GaAs studied by pulsed ion beams

L. B. Bayu Aji,[1,a)] J. B. Wallace,[1,2] and S. O. Kucheyev[1]
[1]*Lawrence Livermore National Laboratory, Livermore, California 94550, USA*
[2]*Department of Nuclear Engineering, Texas A&M University, College Station, Texas 77843, USA*

(Received 30 April 2018; accepted 13 June 2018; published online 9 July 2018)

Gallium arsenide under ion bombardment at room temperature and above exhibits pronounced dynamic annealing that remains poorly understood. Here, we use a pulsed beam method to study radiation defect dynamics in GaAs in the temperature range of 20–100 °C irradiated with 500 keV Xe ions. Results show that, with increasing temperature, the defect relaxation time constant monotonically decreases from ~5.2 to ~0.4 ms. A change in the dominant dynamic annealing process occurs at a critical temperature of ~60 °C, as evidenced by a change in the activation energy. A comparison with the other semiconductors studied by the pulsed beam method (Si, Ge, and 4*H*-SiC) reveals that both the high-temperature activation energy and the temperature below which dynamic annealing becomes negligible scale with the melting point. *Published by AIP Publishing.*
https://doi.org/10.1063/1.5038018

I. INTRODUCTION

Gallium arsenide (GaAs) is a direct bandgap semiconductor attractive for a variety of opto-electronic[1] and photovoltaic[2] devices. Because ion bombardment is the preferred tool for selective-area doping, etching, and defect engineering of semiconductors,[3] radiation-induced defects in GaAs have been a subject of extensive previous investigations.[4–11] Radiation damage in GaAs is complicated by pronounced dynamic annealing (DA), which refers to processes of migration, recombination, and clustering of mobile point defects during irradiation. In fact, GaAs is a prototypical material with strong DA at temperatures (*T*s) close to room *T*.[10]

Despite numerous previous studies,[4–11] the current understanding of DA in GaAs is still very limited. A number of very basic questions remain unanswered. For example, what are the characteristic lifetimes (τ) and diffusion lengths (L_d) of the point defects dominating DA after the thermalization of ballistic collision cascades? Here, we use a recently developed pulsed ion beam method[12–14] to answer these questions. Our results reveal τ values of 5.2–0.4 ms at 20–100 °C and an L_d of ~86 nm at 60 °C for the case of bombardment with 500 keV Xe ions. Furthermore, the $\tau(T)$ dependence points to a change in the dominant DA process at ~60 °C, exhibited by a large change in the DA activation energy. Interestingly, this behavior is qualitatively similar to that for elementary semiconductors such as Si and Ge and different from that for another compound semiconductor, 4*H*-SiC, previously studied by the pulsed beam method. These results have important implications for understanding radiation defect dynamics and developing physics-based models of radiation damage accumulation in materials.

II. EXPERIMENTAL

Single crystals of undoped (100) GaAs were bombarded in the *T* range of 20–100 °C with 500 keV $^{129}Xe^{+}$ ions at 7° off the [100] direction. To improve thermal contact, samples were attached to a Cu sample holder with conductive Ag paste. The 4 MV ion accelerator (National Electrostatics Corporation, model 4UH) at Lawrence Livermore National Laboratory was used for both ion irradiation and ion beam analysis. All irradiations were performed in a broad beam mode.[12] Irradiated areas were $4 \times 5\,mm^2$. Total doses (Φs) were in the range of $(1–3) \times 10^{13}$ ions cm^{-2}.

Ion beam pulsing was achieved by applying high voltage pulses to a pair of parallel plates to deflect the ion beam off the target so that the total Φ was split into a train of equal square pulses with a dose per pulse of $\Phi_{pulse} = F_{on}t_{on}$. The adjacent pulses were separated by time t_{off} (see the inset in Fig. 1). For τ measurements, F_{on} was $1.9 \times 10^{13}\,cm^{-2}\,s^{-1}$, t_{on} was 0.2 ms, and t_{off} was varied between 0.1 and 100 ms.

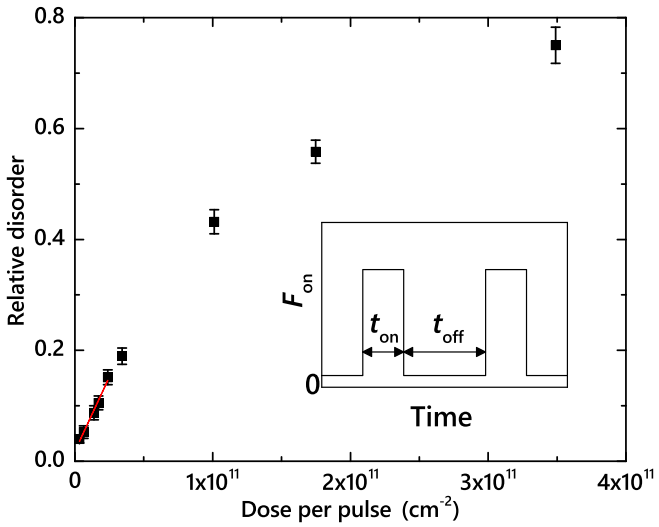

FIG. 1. Relative average bulk disorder in GaAs bombarded at 60 °C with a pulsed beam of 500 keV Xe ions with $F_{on} = 3.4 \times 10^{13}\,cm^{-2}\,s^{-1}$ and $t_{off} = 70$ ms to the same total Φ of $1.5 \times 10^{13}\,cm^{-2}$ as a function of Φ_{pulse}. Linear fitting, shown by the solid line, gives an L_d of 86 ± 14 nm. The inset is a schematic of the time dependence of the instantaneous dose rate for pulsed beam irradiation, defining t_{on}, t_{off}, and F_{on}.

a)Electronic mail: bayuaji1@llnl.gov

TABLE I. Summary of the irradiation conditions analyzed in this work. Also given are materials' melting points (T_{melt}),[23] high- and low-T activation energies of DA (E_a^{HT} and E_a^{LT}), a critical temperature of the change in the dominant DA process (T_c), a cutoff temperature below which DA becomes negligible (T_0), and the temperature range of DA (ΔT) for materials irradiated with 500 keV pulsed ion beams.

Target	Ion	F_{on} (10^{13} cm^{-2} s^{-1})	t_{on} (ms)	E_a^{LT} (eV)	E_a^{HT} (eV)	T_c (°C)	T_o (°C)	ΔT (°C)	T_{melt} (°C)
GaAs	Xe	1.9	0.2	0.11 ± 0.01	0.62 ± 0.09	60	–84 ± 10	144 ± 10	1238
GaAs	Ar	1.4	1.0		0.46 ± 0.08	<60			1238
Si	Ar	1.9	1.0	0.12 ± 0.01	0.42 ± 0.01	60	–88 ± 11	148 ± 11	1414
Ge	Ar	1.5	1.0	0.19 ± 0.05	1.05 ± 0.04	128	–154 ± 19	282 ± 19	938
4*H*-SiC	Ar	1.7	1.0	0.22 ± 0.05		100	–62 ± 28	162 ± 28	2730

For L_d measurements, F_{on} was 3.4×10^{13} cm^{-2} s^{-1}, t_{off} was 70 ms (which, as will be shown below, is much greater than τ), and t_{on} was varied between 0.1 and 5 ms. Possible effects of the collision cascade density were evaluated by additional τ measurements for bombardment at 20, 40, and 60 °C with 500 keV $^{40}Ar^+$ ions with $F_{on} = 1.4 \times 10^{13}$ cm^{-2} s^{-1} and $t_{on} = 1$ ms. Table I summarizes the irradiation conditions used.

The dependence of lattice damage on t_{off} and t_{on} was studied *ex situ* at room T by ion channeling. Depth profiles of lattice disorder were measured with 2 MeV $^4He^+$ ions incident along the [100] direction and backscattered into a detector at 165° relative to the incident beam direction. Spectra were analyzed with one of the conventional algorithms[15] for extracting the effective number of scattering centers (referred to below as "relative disorder"). Values of average bulk disorder (n) were obtained by averaging depth profiles of relative disorder over 10 channels (~25 nm) centered on the maximum of the bulk damage peak. Error bars of n are standard deviations. Ion Φs in τ measurements at different Ts were chosen such that, for continuous beam irradiation, n was in the range of 0.5–0.9 (with $n = 1$ corresponding to full amorphization).

III. RESULTS AND DISCUSSION

A. Diffusion lengths

Pulsed-beam measurements of L_d are based on the analysis of $n(t_{on})$ dependencies.[13,14,16,17] Figure 2(a) plots representative depth profiles of relative disorder in GaAs bombarded at 60 °C with pulsed beams of 500 keV Xe ions to the same total Φ, with $t_{off} = 70$ ms and with three different t_{on} values. It is seen that the damage level throughout the implantation depth increases with increasing t_{on} when all the other irradiation parameters are kept constant. This trend is better illustrated in Fig. 1, where n is plotted as a function of Φ_{pulse}. As discussed in detail previously,[13,14,16,17] for $t_{off} \gg \tau$, the interaction between mobile defects generated in different pulses is suppressed, and the $n(\Phi_{pulse})$ dependence reflects the interaction of mobile defects created in different cascades within the same pulse.

Furthermore, for $t_{on} < \tau$, the majority of defect relaxation occurs during the passive (t_{off}) rather than active (t_{on}) portion of the beam duty cycle. Hence, the average density of ion-beam-generated mobile point defects after each pulse can be expressed as $\rho_{displacement} \propto 1 + 4L_d^2 F_{on} t_{on}$.[14] For low t_{on} values, an assumption of $n \propto \rho_{displacement}$ can be made,[14] and a linear fit of the $n(\Phi_{pulse})$ dependence (the solid line in Fig. 1) yields $L_d = 86 \pm 14$ nm. Interestingly, this is larger than L_d values of 5–50 nm measured for Si, Ge, and SiC.[13,14,17,18] A larger L_d is, however, consistent with the observation (Fig. 2) that the defect dynamics affects the entire implantation range, from the sample surface to the end of ion range region. This is in contrast to results for Si, Ge, and SiC where the near-surface region with a thickness comparable with L_d exhibits suppressed DA, with the near-surface damage level being essentially independent of the pulsing parameters t_{on} and t_{off}.

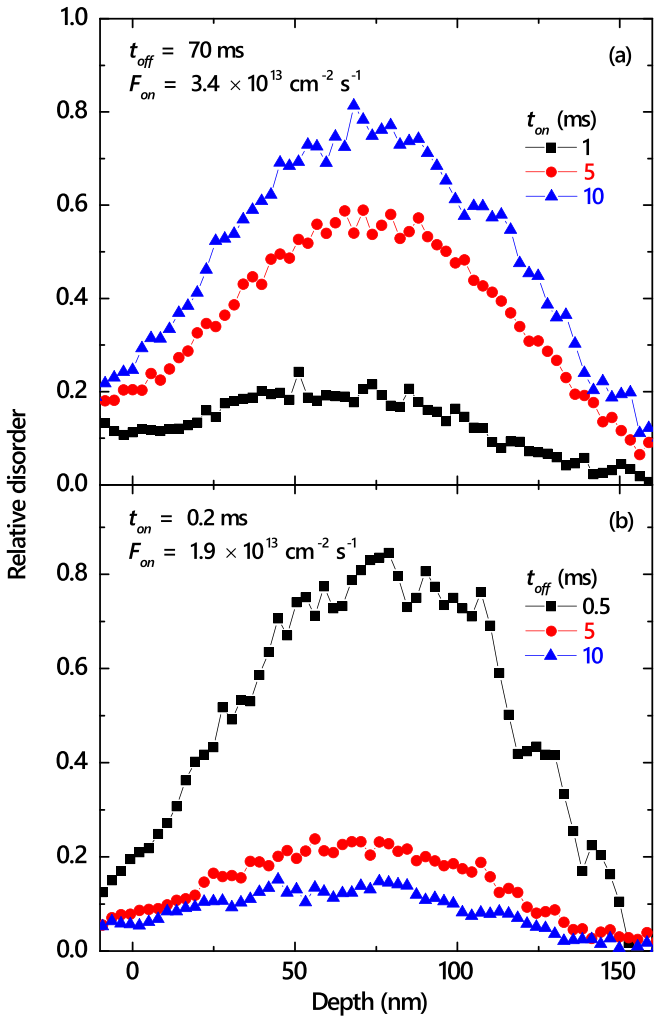

FIG. 2. Selected depth profiles of relative disorder in GaAs bombarded at 60 °C with a pulsed beam of 500 keV Xe ions with F_{on}, t_{on}, and t_{off} given in the legends at total Φs of (a) 1.5×10^{13} cm^{-2} and (b) 2×10^{13} cm^{-2}. For clarity, only every 3rd experimental point is depicted. Panel (a) is a pulsed beam measurement of L_d, whereas (b) is a measurement of τ.

B. Defect lifetimes

Pulsed-beam measurements of τ are based on the analysis of $n(t_{off})$ decay curves.[12,14] Fig. 2(b) shows three representative damage–depth profiles for bombardment at 60 °C with different t_{off} values, and all the other irradiation conditions kept constant. In these measurements of τ, the Φ_{pulse} is chosen to minimize the interaction of mobile defects generated in different pulses, while maximizing the inter-pulse defect interaction. This occurs when, on average, only one ion impacts onto L_d-defined areas during each pulse or when $t_{on} = \frac{1}{4L_d^2 F_{on}}$.[13] For $F_{on} = 1.9 \times 10^{13}\,\mathrm{cm^{-2}\,s^{-1}}$ and $L_d = 86$ nm, this condition is satisfied when $t_{on} = 0.2$ ms. Hence, we have used $t_{on} = 0.2$ ms in all the $n(t_{off})$ measurements with Xe ions. It is seen from Fig. 2(b) that the damage level throughout the implantation depth monotonically decreases with increasing t_{off}. Figure 3 summarizes all the $n(t_{off})$ dependencies measured at different Ts. Solid lines in Fig. 3 are fits of the data via the Marquardt-Levenberg algorithm[19] with the first order decay equation $[n(t_{off}) = n_\infty + (n_0 - n_\infty)\exp(-t_{off}/\tau)]$. Here, n_∞ is n for $t_{off} \gg \tau$. Figure 4 (left axis) shows fitting results, with τ values in the range of ~0.4–5.2 ms, monotonically increasing with decreasing T from 100 to 20 °C. It is interesting to compare results of Fig. 4 with the two τ values measured in previous 500 keV Xe pulsed-beam studies of other semiconductors, Si ($\tau = 14$ ms for Si vs 5.2 ms for GaAs at 20 °C)[13] and 3*C*-SiC ($\tau = 5$ ms for SiC vs 0.4 ms for GaAs at 100 °C).[20] We see that, in both cases, GaAs exhibits much smaller τ values. This finding is, however, not unexpected, given that DA processes are strongly material-dependent.

Also plotted in Fig. 4 (right axis) is the T dependence of the DA efficiency (ξ), which we define as before:[12–14] $\xi = \frac{n(0)-n_\infty}{n(0)}$. Figure 4 shows that ξ increases with T close-to-linearly up to a T_c of ~60 °C and then approaches a saturation of ~95% for higher Ts. The low-T linear portion of the $\xi(T)$ dependence can be expressed as $\xi(T) = \frac{T-T_0}{\Delta T}$, with T_0 and ΔT as the fitting parameters. The fitting is shown by a solid line in Fig. 4. It predicts that the DA will vanish (i.e., $\xi \to 0$) at Ts below a T_0 of –84 °C, with the DA range between T_0 and T_c of ΔT ~144 °C.

In order to gain insight into DA mechanisms, Fig. 5 shows the $\tau(T)$ dependency from Fig. 4 replotted in Arrhenius coordinates, with the DA rate defined as $\frac{1}{\tau}$, and with $k_B T$ having the usual meaning. Two Arrhenius regimes are clearly seen, one below and one above a critical transition temperature of $T_c \sim 60$ °C. Note that this T_c coincides with the T when the $\xi(T)$ dependence appears to saturate in Fig. 4. Such a correlation of T_c from the Arrhenius plot of

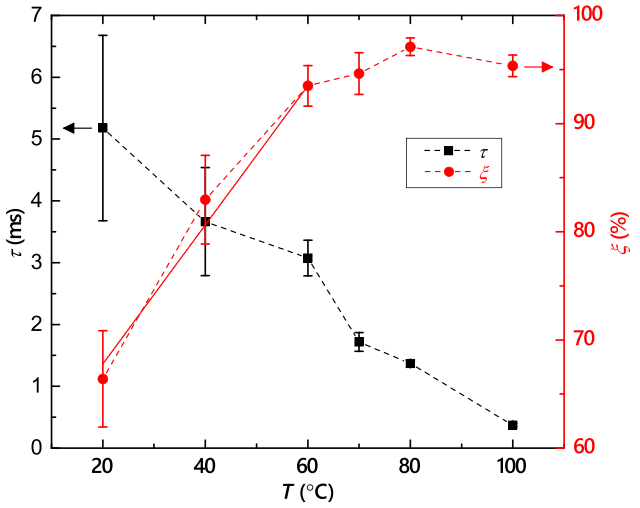

FIG. 4. Temperature dependencies of (left axis) the DA time constant (τ) and (right axis) the DA efficiency (ξ) for GaAs bombarded with 500 keV Xe ions. Linear fitting of the $\xi(T)$ dependence, shown by the solid line, yields the cutoff temperature (T_0) below which DA is negligible and the temperature range of DA (ΔT).

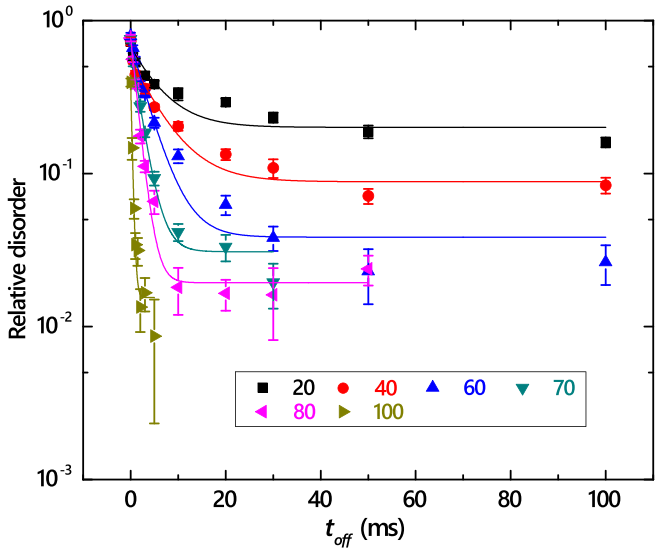

FIG. 3. Relative average bulk disorder in GaAs bombarded with pulsed beams of 500 keV Xe ions with $F_{on} = 1.9 \times 10^{13}\,\mathrm{cm^{-2}\,s^{-1}}$ and $t_{on} = 0.2$ ms as a function of the passive portion of the beam duty cycle (t_{off}) at different Ts given in the legend (in °C). Fitting curves with the first order decay equation are shown by solid lines.

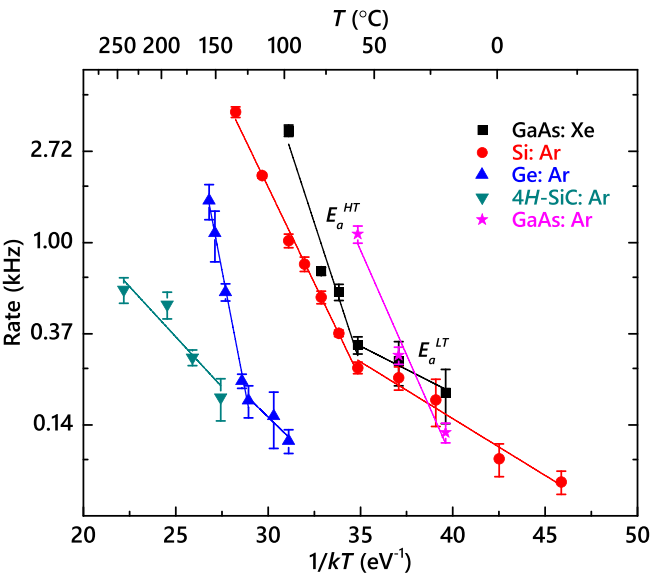

FIG. 5. Arrhenius plot of the DA rate (defined as $1/\tau$) for four different materials bombarded with either 500 keV Ar or 500 keV Xe ions, as indicated in the legend. Data for GaAs are from the present work, while results for the other materials are taken from Refs. 12, 14, and 23.

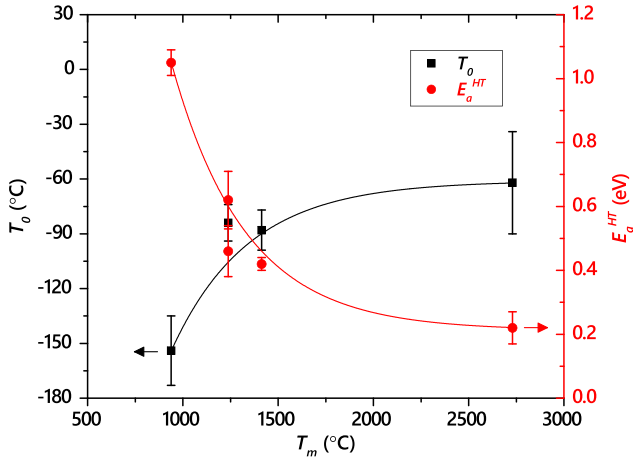

FIG. 6. Dependence of (left axis) T_0 and (right axis) E_a^{HT} on the melting temperature for the four materials studied by the pulsed beam method. Data for GaAs is from the present work, while results for the other materials are taken from Refs. 12, 14, and 23. Solid lines are to guide the eye.

the DA rate and the saturation T of the $\xi(T)$ dependence has also been observed in the previous pulsed beam studies of Si and Ge.[14,21] Linear fitting of the data in Fig. 5 gives two activation energies of $E_a^{HT} = 0.62 \pm 0.09$ eV and $E_a^{LT} = 0.11 \pm 0.01$ eV, above and below a T_c of 60 °C, respectively. Figure 5 also shows the three data points that we have measured for GaAs bombarded at 20, 40, and 60 °C with 500 keV Ar ions. It reveals that both E_a^{HT} and T_c appear to depend on ion mass (and, hence, the cascade density) as the Arrhenius plot for the case of Ar ion bombardment is offset to lower Ts with E_a^{HT} of 0.45 ± 0.07 eV. Future studies are needed to better understand such cascade-density effects on radiation defect dynamics in GaAs.

Also plotted in Fig. 5 are DA rates for Si, Ge, and 4*H*-SiC obtained by the analysis of data published previously[12,14,22] for bombardment with 500 keV Ar ions. Table I summarizes the radiation defect dynamics parameters measured by the pulsed beam method for these materials. It is seen from Fig. 5 and Table I that E_a^{HT} and the cutoff T of DA (T_0) scale with the melting point. This is better illustrated by Fig. 6. The scaling of T_0 with the melting point is not unexpected. Indeed, DA is related to defect mobility, which is expected to increase when T approaches the material's melting point. The physics behind a decrease in E_a^{HT} with increasing melting point is less clear. It could be related to the fact that the melting point reflects the bond energy in the material, given that DA processes are expected to be more efficient in materials with larger energy bonds, resulting in a larger energy gain upon defect annihilation and the recovery of broken or distorted bonds. These results deserve future modeling effort to correlate the E_a values measured with specific defect migration and interaction processes.

IV. CONCLUSIONS

In summary, we have used the pulsed beam method to study defect interaction dynamics in GaAs bombarded in the T range of 20–100 °C with 500 keV Xe ions. Results have revealed that the characteristic time constant of dynamic annealing decreases monotonically from 5.2 to 0.4 ms with increasing T. We have estimated a defect diffusion length of 86 ± 14 nm at 60 °C. There is a characteristic change in the dominant DA process at ~60 °C, characterized by a major change in the activation energy from ~0.1 to ~0.6 eV. The details of radiation defect dynamics revealed in this work have important implications for predicting radiation response in regimes with strong DA and could be used to benchmark models of damage accumulation in GaAs-based electronic devices.

ACKNOWLEDGMENTS

This work was funded by the Nuclear Energy Enabling Technology (NEET) Program of the U.S. DOE, Office of Nuclear Energy, and performed under the auspices of the U.S. DOE by LLNL under Contract No. DE-AC52-07NA27344. J.B.W. would like to acknowledge the LGSP for funding.

[1]S. Mokkapati and C. Jagadish, "III-V compound semiconductors for optoelectronic devices," Mater. Today **12**, 22 (2009).
[2]M. Bosi and C. Pelosi, "The potential of III-V semiconductors as terrestrial photovoltaic devices," Prog. Photovoltaics **15**, 51 (2007).
[3]J. S. Williams, "Ion implantation of semiconductors," Mater. Sci. Eng. A **253**, 8 (1998).
[4]E. Wendler, W. Wesch, and G. Götz, "Influence of the dose rate on the damage production in ion implanted GaAs," Nucl. Instrum. Methods Phys. Res. Sect. B **52**, 57 (1990).
[5]W. H. Weisenberger, S. T. Picraux, and F. L. Vook, "Low temperature channeling measurements of ion implantation lattice disorder in GaAs," Rad. Eff. **9**, 121 (1971).
[6]C. R. Musil, J. Melngailis, S. Etchin, and T. E. Haynes, "Dose-rate effects in GaAs investigated by discrete pulsed implantation using a focused ion beam," J. Appl. Phys. **80**, 3727 (1996).
[7]N. A. G. Ahmed, C. E. Christodoulides, and G. Carter, "Flux, fluence and implantation temperature dependence of disorder produced by 40 keV N^+ ion irradiation of GaAs," Radiat. Eff. **52**, 211 (1980).
[8]T. E. Haynes and O. W. Holland, "Comparative study of implantation-induced damage in GaAs and Ge: Temperature and flux dependence," Appl. Phys. Lett. **59**, 452 (1991).
[9]T. E. Haynes and O. W. Holland, "Dose rate effects on damage formation in ion-implanted gallium arsenide," Nucl. Instrum. Methods Phys. Res. Sect. B **59/60**, 1028 (1991).
[10]R. A. Brown and J. S. Williams, "Critical temperature and ion flux dependence of amorphization in GaAs," J. Appl. Phys. **81**, 7681 (1997).
[11]R. A. Brown and J. S. Williams, "Crystalline-to-amorphous phase transformation in ion-irradiated GaAs," Phys. Rev. B **64**, 155202 (2001).
[12]M. T. Myers, S. Charnvanichborikarn, L. Shao, and S. O. Kucheyev, "Pulsed ion beam measurement of the time constant of dynamic annealing in Si," Phys. Rev. Lett. **109**, 095502 (2012).
[13]J. B. Wallace, S. Charnvanichborikarn, L. B. Bayu Aji, M. T. Myers, L. Shao, and S. O. Kucheyev, "Radiation defect dynamics in Si at room temperature studied by pulsed ion beams," J. Appl. Phys. **118**, 135709 (2015).
[14]J. B. Wallace, L. B. Bayu Aji, L. Shao, and S. O. Kucheyev, "Dynamic annealing in Ge studied by pulsed ion beams," Sci. Rep. **7**, 13182 (2017).
[15]K. Schmid, "Some new aspects for the evaluation of disorder profiles in silicon by backscattering," Radiat. Eff. **17**, 201 (1973).
[16]S. Charnvanichborikarn, M. T. Myers, L. Shao, and S. O. Kucheyev, "Pulsed ion beam measurement of defect diffusion lengths in irradiated solids," J. Phys. Condens. Matter **25**, 162203 (2013).
[17]L. B. Bayu Aji, J. B. Wallace, L. Shao, and S. O. Kucheyev, "Effective defect diffusion lengths in Ar-ion bombarded 3C-SiC," J. Phys. D Appl. Phys. **49**, 19LT01 (2016).
[18]J. B. Wallace, L. B. Bayu Aji, L. Shao, and S. O. Kucheyev, "Fractal analysis of collision cascades in pulsed-ion-beam-irradiated solids," Sci. Rep. **7**, 17574 (2017).
[19]K. Levenberg, "A method for the solution of certain problems in least squares," Q. Appl. Math. **2**, 164 (1944).

[20]L. B. Bayu Aji, J. B. Wallace, L. Shao, and S. O. Kucheyev, "Effects of collision cascade density on radiation defect dynamics in 3C-SiC," Sci. Rep. **7**, 44703 (2017).
[21]J. B. Wallace, L. B. Bayu Aji, A. A. Martin, S. J. Shin, L. Shao, and S. O. Kucheyev, "The role of Frenkel defect diffusion in dynamic annealing in ion-irradiated Si," Sci. Rep. **7**, 39754 (2017).
[22]L. B. Bayu Aji, J. B. Wallace, L. Shao, and S. O. Kucheyev, "Non-monotonic temperature dependence of radiation defect dynamics in silicon carbide," Sci. Rep. **6**, 30931 (2016).
[23]*CRC Handbook of Chemistry and Physics*, 98th ed., edited by J. R. Rumble (CRC Press, Taylor & Francis, Boca Raton, FL, 2018) (Internet Version).